Climate Change and Downstream Water Quality in Agricultural Production: The Case of Nutrient Runoff to the Gulf of Mexico

Levan Elbakidze[a,b*]
Associate Professor
levan.elbakidze@mail.wvu.edu

Yuelu Xu[a]
Post-Doctoral Fellow
yuelu.xu@mail.wvu.edu

Philip W. Gassman[c]
Associate Scientist
pwgassma@iastate.edu

Jeffrey G. Arnold[d]
Agricultural Engineer
jeff.arnold@usda.gov

Haw Yen[e,f]
Senior Scientist
haw.yen@gmail.com

[a] Division of Resource Economics and Management, Davis College of Agriculture, Natural Resources and Design, West Virginia University, Agricultural Sciences Building, Morgantown, West Virginia 26506, USA.
[b] Center for Innovation in Gas Research and Utilization, West Virginia University, Morgantown, West Virginia 26506, USA.
[c] Center for Agricultural and Rural Development, Iowa State University, Ames, Iowa 50011, USA.
[d] Grassland Soil and Water Research Laboratory, USDA-ARS, Temple, Texas 76502, USA.
[e] Crop Science, Bayer U.S., 700 W Chesterfield Pkwy W, Chesterfield, Missouri 63017, USA.
[f] School of Forestry & Wildlife Science, Auburn University, Auburn, Alabama 36849, USA.
[*]Corresponding author

Abstract

Nitrogen (N) fertilizer use in agricultural production is a significant determinant of surface water quality. As climate changes, agricultural producers are likely to adapt at extensive and intensive margins in terms of planted acreage and per ha input use, including fertilizers. These changes can affect downstream water quality. We investigate the effect of climate-driven land productivity changes on water quality in the Gulf of Mexico using an integrated hydro-economic agricultural land use (IHEAL) model. Our results indicate that land and N use adaptation in agricultural production to climate change increases N delivery to the Gulf of Mexico by 0.5%-1.6% (1,690 -5,980 metric tons) relative to the baseline scenario with no climate change.

1. Introduction

Mississippi River Basin (MRB) spans more than 3.2 million square kilometers, is dominated by agricultural land use, and is the largest drainage basin in the U.S. Approximately 70% of U.S. cropland is in the MRB (Kumar and Merwade, 2011; Marshall et al., 2018). Agricultural production in the MRB relies on intensive nitrogen (N) fertilizer use with a well-documented negative externality in the form of Hypoxia in the Gulf of Mexico.

Hypoxia in the Gulf has been a public concern for decades due to the detrimental consequences for the aquatic ecosystems (US EPA, 2019). N runoff to the Gulf and the consequent eutrophication of coastal waters promotes algal bloom. Decomposing algae depletes the marine ecosystem of dissolved oxygen, which is critical for sustaining aquatic ecosystems. Oxygen depletion results in hypoxic or “dead” zones as marine life either dies or migrates to other areas. In 2001, the EPA established the Gulf of Mexico Hypoxia Task Force to reduce the size of the Hypoxic zone to 5,000 km^2 by 2035 (US EPA, 2014). In 2021, the hypoxic zone in the Gulf still reached 16,405 km^2, significantly exceeding the EPA goal (US EPA, 2021a).

Climate change, with higher temperatures, more variable rainfall, and elevated

CO_2 concentrations, can substantially affect crop yields and agricultural production. Previous literature documents mixed expected impacts of climate change on crop yields in the MRB. Panagopoulos et al. (2014) simulated corn and soybean yields in the Upper Mississippi River Basin (UMRB, a subbasin of the MRB) using the Soil and Water Assessment Tool (SWAT) for the baseline climate (1981-2000) and seven future (2046-2065) GCM climate projections under four agricultural management scenarios. Predicted corn and soybean yields modestly decline relative to the baseline climate conditions under all future climates and agricultural management scenarios. Panagopoulos et al. (2015) reported similar results for the Ohio-Tennessee River Basin (OTRB, a subbasin of the MRB), with predicted corn and soybean yields in all examined future climates and agricultural management practices declining relative to the corresponding baseline scenarios. Chen et al. (2019) modeled the effects of climate change on crop yields in the Northern High Plains of Texas (partially located within the MRB) using the SWAT. They found that the median irrigated corn and sorghum yields would decrease by 3%-22% and 6%-42%, respectively, relative to the historical values. Median non-irrigated sorghum yield would decrease by up to 10%.

The changes in crop yields in the MRB may influence agricultural input and land use with associated implications for environmental outcomes in the Gulf of Mexico. On the one hand, the use of N fertilizer may intensify to compensate for losses in crop yields. This may increase N runoff from the MRB and exacerbate Hypoxia in the Gulf of Mexico. On the other hand, lower yields may reduce profitability of crop production and may result in decreased crop acreage, which could decrease N runoff to the Gulf of Mexico. The net effect of climate change-driven changes in crop yields on N runoff to the Gulf of Mexico is thus unclear and should be examined empirically.

The MRB is the largest basin in the U.S. and includes several large sub-basins with different agricultural practices and contributions to the Gulf N runoff. For example, UMRB and OTRB are major N contributors to the Gulf (Kling et al., 2014;

White et al., 2014). In the Corn Belt, highly fertile soils, relatively level land, hot days and nights, and well-distributed precipitation during the growing season provide ideal conditions for crop production (Wu et al., 2015). These factors have led to prevalent corn-soybean rotation with high fertilizer use and tile drainage systems. The Missouri and Arkansas-Red-White River Basin includes both rainfed and irrigated crop production. In Nebraska, western Kansas, Oklahoma and north Texas, groundwater from Ogallala aquifer is a major source of irrigation for agricultural production (Xu et al. 2022). Some of the climate projection scenarios suggest that regions with rainfed agriculture will be wetter and regions relying on irrigation will be drier (NCAR, 2022a). These spatially heterogeneous changes, and the corresponding adaptations, are important to examine in terms of implications for environmental outcomes.

The MRB contains 962,342 square kilometers of cropland. Corn, soybean, and wheat are dominant crops, which account for 34.6%, 23.1%, and 18.0% of cropland, respectively (Marshall et al., 2018). Figure 1 presents the harvested acreages of major crops planted in the MRB from 1997 to 2017 (USDA NASS, 2019). Corn and soybean acreages increased substantially over time mainly due to the increasing demand for feedstock sources in bioenergy production and feed for both domestic and overseas livestock operations (USDA ERS, 2022). Meanwhile, wheat and sorghum acreages have decreased. Correspondingly, irrigated corn and soybean acreages grew significantly from 1997 to 2017, while irrigated wheat and sorghum acreages declined (Figure 2).

There are several farmer adaptation options to climate-driven changes in crop yields. For example, technological developments, government and insurance programs, alternative farm production practices like new irrigation systems, and more drought tolerant crops can mitigate some of the climate impacts on agriculture (Smit and Skinner, 2002). While these options are important for a comprehensive examination, in this study, we offer a partial analysis of farmers' response to climate driven changes in crop yields. We examine adaptation at the extensive (planting decisions for existing crops) and intensive (per ha nitrogen use and irrigation) margins, ceteris paribus. This analysis offers an initial assessment of the relationship between N runoff and adaptation in agricultural production to climate change. Future studies should consider a wider set of adaptation alternatives including new crop varieties and production technologies.

While there is extensive literature on the impacts of agricultural production on N loading in surface water, few studies have evaluated this problem in the context of climate change. Bosch et al. (2018) and Xu et al. (2019) evaluated the effects of climate change on the costs of achieving water quality goals in an experimental watershed in Pennsylvania using an economic model and the SWAT-Variable Source Area model with climate predictions. Both studies showed that estimated costs of meeting water quality goals increase in future climates relative to the historical baseline. However, N fertilizer use in these studies is exogenously determined, which limits N use flexibility in response to variations in crop yields in future climate scenarios.

We contribute to previous literature by examining the effects of climate change on N runoff to the Gulf of Mexico with endogenous land and N use decisions. Our approach includes a behavioral crop production response to changes in productivity and evaluates N runoff accordingly. Our focus is on N and land use with associated impacts on N runoff to the Gulf, as a response to crop yield changes in future climate scenarios. Our primary purpose is to draw attention to the implications of adaptation to climate change in agricultural production for N use and downstream water quality. This aspect of climate change and associated adaptation has not received much attention in scientific literature. It is important to note that the objective of this study is not to predict the changes in N runoff to the Gulf under a changing climate, as the modeling exercise is based on several important assumptions and limitations that we discuss in the conclusions section. Instead, our goal is to provide a first, partial assessment of the sensitivity of Gulf N runoff to the changes in crop yields and corresponding adaptation in crop production for some mid-century (2050-2068) climate change scenarios. The results of this study should encourage additional analysis of changes in N runoff as an externality from agricultural production adaptation to climate change.

2. Theoretical Framework

This section presents a theoretical economic framework and simplified analytical results illustrating the impact of climate driven changes in crop yields on fertilizer use. A parsimonious welfare maximization model with a representative commodity market is considered as:

$$\max_{x,n_1,n_2,w_1} \pi = \int_0^{\mathrm{x}} \mathrm{p}(t)\,dt - C_n * (n_1 + n_2) - C_w * w_1 \quad (1)$$

subject to

$$\alpha_1 * f(n_1, w_1) + \alpha_2 * g(n_2) \geq \mathrm{x} \quad (2)$$

where x is crop consumption $\mathrm{p}(t)$ is the inverse commodity demand function. C_n and C_w are unit costs for fertilizer and water, respectively. Crop production takes place in irrigated region 1 and rainfed region 2. $f(n_1, w_1)$ is production function in region 1 requiring nitrogen (n_1) and water (w_1) as input factors, with $f' > 0$, and $f'' < 0$. $g(n_2)$ is production function in region 2 only requiring only nitrogen (n_2), with $g' > 0$, and $g'' < 0$. For example, corn production in Illinois is mostly rainfed, while irrigated corn is prevalent in Kansas and Nebraska. α_1 and α_2 is the yield multiplier in future climates, with $\alpha > 1$ indicating an increase in crop yield and $0 < \alpha < 1$ indicating a reduction in crop yield. Equations (2) limits crop consumption to not exceed production.

The appendix provides the Lagrangian and the first-order conditions, which are used to form the Hessian matrix. The determinant of the Hessian matrix is:

$$
\begin{aligned}
|H| = \alpha_1{}^2\alpha_2\lambda^2 \Big[& 2\alpha_1 f_{n_1} f_{n_1w_1} f_{w_1} g_{n_2n_2} p_x - \alpha_1 f_{n_1}{}^2 f_{w_1w_1} g_{n_2n_2} p_x \\
& + f_{n_1w_1}{}^2 \left(\lambda g_{n_2n_2} + \alpha_2 p_x g_{n_2}{}^2\right) \\
& - f_{n_1n_1}\left(\lambda f_{w_1w_1} g_{n_2n_2} + \alpha_2 f_{w_1w_1} p_x g_{n_2}{}^2 + \alpha_1 f_{w_1}{}^2 g_{n_2n_2} p_x\right)\Big]
\end{aligned}
$$

Comparative statics for changes in variables of interest with respect to the change in α_1 are obtained using Cramer's rule:

$$
\frac{\partial n_1}{\partial \alpha_1} = \frac{-\alpha_1\alpha_2\lambda^2\left(f_{n_1w_1}f_{w_1} - f_{n_1}f_{w_1w_1}\right)\left(\alpha_2 p_x g_{n_2}{}^2 + g_{n_2n_2}\left(\lambda + \alpha_1 p_x f(n_1, w_1)\right)\right)}{|H|} \quad (3)
$$

$$
\frac{\partial n_2}{\partial \alpha_1} = \frac{-\alpha_1{}^2\alpha_2\lambda^2 g_{n_2} p_x\left[-2 f_{n_1} f_{n_1w_1} f_{w_1} + f_{n_1n_1} f_{w_1}{}^2 + f(n_1, w_1)\left(f_{n_1w_1}{}^2 - f_{n_1n_1} f_{w_1w_1}\right)\right]}{|H|} \quad (4)
$$

$$
\frac{\partial w_1}{\partial \alpha_1} = \frac{-\lambda^2\alpha_1\alpha_2\left(f_{n_1w_1}f_{n_1} - f_{w_1}f_{n_1n_1}\right)\left(\alpha_2 p_x g_{n_2}{}^2 + g_{n_2n_2}\left(\lambda + \alpha_1 p_x f(n_1, w_1)\right)\right)}{|H|} \quad (5)
$$

The denominator $|H|$ in equations (3), (4) and (5) is positive according to the maximization requirements. Therefore, the sign of equation (3), which shows the effects of changes in crop yields in region 1 on the N use in region 1, depends on the signs of the numerator. The direction of the derivative is indeterminate and depends on the slope of the demand curve, production function, change in yield, and price of the commodity. The sign of equation (4), indicating the effects of changes in crop yields in region 1 on N use in region 2, is also ambiguous and depends on the relative magnitudes of commodity price, yield and yield changes with respect to irrigation and fertilizer, and slope of the demand curve. Similar results can be observed for productivity changes in region 2 (α_2) and are provided in the appendix. Since nutrient runoff to the Gulf depends on per ha use of N and on acreage decisions, the combined effect of changes in productivity (α) on N runoff is ambiguous.

The sign of equation (5), which shows the effects of changes in crop yields in region 1 on water use in region 1, is also ambiguous. The direction of the change in water use in region 1 under climate change depends on the production function, the price of the commodity, and magnitudes of changes in both crop yields. Similar results hold for the effect of region to yield changes (α_2) on water use in region 1 (see appendix).

The simplified analytical model provides a theoretical insight for the effect of altered crop yields on input use as a form of adaptation to climate change. The result shows theoretical foundations for the need to consider the behavioral response to climate change alongside biophysical parameters in assessing the impacts of changes in production environment on production decisions that generate externalities for downstream water quality. Economic factors including prices and demand, and biophysical production parameters determine the first order conditions. Therefore, rigorous assessments of changes in N runoff from agricultural production in response to climate change should combine biophysical and economic modeling systems that account for adaptation in production activities. For the sake of parsimony, the theoretical analysis only considers two regions and a representative commodity rather than a set of crops, which is important to consider empirically as relocation of crop production will alter spatial N use distribution and runoff to the Gulf. In the empirical analysis, we use a spatially explicit model with four N intensive crops that combines biophysical and economic components to examine changes in N runoff.

3. Methods and data

We use the IHEAL model (Xu et al., 2022) to empirically assess the effects of climate change-driven crop yield variation on N runoff to the Gulf of Mexico. IHEAL is an integrated hydro-economic agricultural land use model, which combines a national price endogenous partial equilibrium commodity market formulation for select crops and a process-based SWAT. Corn, soybean, wheat and sorghum are included in the model as individual commodities because these crops are the most fertilizer-intensive crops planted in the U.S. (USDA NASS, 2020; Marshall et al., 2015; Steiner et al., 2021). Production of all other commodities is combined to account for county-scale agricultural land use. The model includes county-scale crop planting, fertilizer use, and irrigation decisions. Production activities generate national commodity supply estimates that are combined with corresponding national commodity demand functions to produce equilibrium prices, quantities, and producer and consumer surplus estimates. The model endogenously determines annual county crop planting acreage, N use, and irrigation based on constrained consumer and producer welfare maximization in the select crop markets.

The IHEAL model maximizes consumer and producer welfare in the U.S. subject to commodity specific supply-demand balance, including exports and imports, production technology constraints, irrigated acreage constraints, and land allocation constraints that represent a convex combination of historically observed and synthetic county crop acreages. Historical and synthetic crop acreage proportions at the county scale are used to constrain planting decisions, so that model solutions reflect agronomic, managerial and technologic requirements for crop rotation. Synthetic acreages are obtained using own and cross-price elasticities and own and cross acreage price elasticities following Chen and Onal (2012). Elasticity estimates are obtained using fixed effect Arellano-Bond estimator and county production and price data from 2005 to 2019.

HAWQS platform is used to obtain SWAT long-run crop yields and N runoff to the Gulf for the baseline time period (2000-2018) (HAWQS, 2020). HAWQS platform also provides future (2050-2068) crop yields for five different Coupled Model Intercomparison Project Phase 5 (CMIP5) climate models, including ACCESS1.3, MIROC5, IPSL-CM5A-LR, MIROC-ESM-CHEM and CCSM4[1]. Table 1 presents the list of climate models used in this study. The performance of the selected climate models is discussed in Harding et al. (2013). Figure 3 presents average crop yields across all counties within the MRB under baseline (historical) and future climate scenarios. The "Ensemble" scenario is the mean across all climate change models.

[1] The climate models in our study were selected based on the availability in HAWQS, and inclusion in Harding et al. (2013) assessment.

The impacts of climate change on corn yields are negative in all climate scenarios relative to the baseline, which is consistent with previous literature (Panagopoulos et al., 2014, 2015; Chen et al., 2019). The impacts on soybean, wheat and sorghum yields are mixed across climate models.

The IHEAL model includes crop production activities in 2,788 counties in the contiguous U.S. where at least one of the crops included in this model was planted in at least one year from 2005 to 2019. These counties include 1,620 that are located within MRB and 1,168 outside. Per ha crop yields in the counties located within MRB are expressed as functions of N use and irrigation using SWAT parameters. Per ha crop yields in counties outside of MRB are fixed based on the USDA data and do not vary with irrigation and N use. Instead, to account for the aggregate impact of climate change on yields outside the MRB, we discount corn, soybean, and sorghum yields by 1.6%, 2.7%, and 6%, respectively, and increase wheat yields by 7% relative to their corresponding baseline values (Basche et al., 2016; Karimi et al., 2017; Chen et al., 2019). County planted acreages within and outside of MRB are endogenously estimated.

The parametric model data include crop demand elasticities, market prices, county-specific historical crop acreage, historical county maximum irrigated acreage, and input costs, including energy, fertilizer, water and other production costs. The crop demand elasticities are obtained from previous literature (Westcott and Hoffman, 1999; Piggott and Wohlgenant, 2002; Ishida and Jaime, 2015). The crop market prices and historical crop acreage are collected from USDA NASS (USDA NASS, 2020). The county maximum observed irrigated acreages are obtained from U.S. Geological Survey data (Dieter et al., 2018; USGS, 2018). The upper bounds on county scale irrigated acreage restrict model solutions from irrigating lands that have never been irrigated due to water, water right, and/or capital limitations. Energy input, fertilizer, water and other production costs are obtained from USDA ERS (USDA ERS, 2019). IHEAL combines county production activities, including crop planting acreage, irrigation, fertilizer use and leaching with the watershed SWAT delivery ratios to estimate annual N runoff from crop production to the Gulf of Mexico (White et al., 2014).

4. Results and discussion

Section 4 is organized as follows. We first present the validation and baseline results. Next, we discuss aggregate MRB results for crop production and N runoff with adjusted crop yields within the MRB under future climate scenarios. Then, we evaluate crop production and N runoff to the MRB under altered precipitation within the MRB and crop yields outside the MRB in future climates. Finally, we present the corresponding spatial results for the changes in N use and delivery to the Gulf of Mexico relative to the baseline values.

4.1 Validation and baseline results

The purpose of this section is twofold. One is to validate the model solutions in terms of replicating observed market data. The other is to obtain baseline estimates of N runoff to the Gulf, to be used as benchmarks for subsequent climate scenario analyses.

For model validation purposes, the model is solved using observed county historical crop mix data. We present the 2018 observed values and the corresponding key baseline model solutions, including crop production, crop prices, the amount of N delivered to the Gulf of Mexico, irrigated crop acreage, and the irrigation water used for corn, soybean, sorghum, and wheat within the MRB as part of model validation (Table 2). The model overestimates cumulative crop acreage for corn, soybean, wheat and sorghum by 10.0%, 8.3%, 9.9% and 4.4%, respectively, relative to the acreages observed in 2018. All estimated crop prices are close to the observed values in 2018, with all deviations less than 3%.

Baseline water use, N use and N delivery to the Gulf of Mexico are also presented in Table 2. The estimated irrigated acreage of corn, soybean, wheat and sorghum within the MRB is 3.92 million ha, representing 65.93% of irrigated acreage for these crops in the U.S. in 2018. The annual water use within the MRB is 4.52 million acre-feet, which accounts for 5.42%[2] of the total observed irrigation water use in the U.S. Annual N use within the MRB for corn, soybean, wheat and sorghum is 6,835 thousand metric tons, which is 54.20% of the total N use in the U.S. The corresponding N delivered to the Gulf of Mexico from fertilizer use in corn, soybean, wheat, and sorghum fields is 370,140 metric tons, accounting for 46.5% of the total N delivered to the Gulf of Mexico from the agricultural sector in the MRB (White et al., 2014). These solutions provide a firm footing and benchmark for the subsequent analysis of N runoff scenarios.

We use the historical and synthetic crop mix data to generate baseline model results as a reference point for comparison to the solutions from the climate change scenarios (column 3, Table 2). Synthetic crop acreages allow for greater model flexibility than the model that uses only historical crop mix. The added flexibility is advantageous for the scenarios with constraints or parameter values that fall outside of historically observed settings. We use these baseline results as benchmarks, rather than the results in column 1, for greater consistency between long-run equilibrium results of scenarios with and without added restrictions. The baseline N runoff to the Gulf of Mexico is 369,190 metric tons.

4.2 Results for future climate scenarios

This section presents the results from the IHEAL model with predicted changes in crop yields within the MRB for 2050-2068. Table 3 shows aggregate MRB results for crop acreage and production, irrigated acreage, water use, N fertilizer use and corresponding runoff to the Gulf of Mexico under baseline and future climates. Results from five climate models, including ACCESS1.3, MIROC5, IPSL-CM5A-LR, MIROC-ESM-CHEM and CCSM4, are presented. Among these models, CCSM4 and IPSL-CM5A-LR scenarios produce the lowest and highest impacts on N runoff to the

[2] This value does not include other irrigation intensive crops like rice and alfalfa grown in the MRB.

Gulf. We focus our discussion of results on these models as these provide the upper and lower bounds for N runoff impacts. In addition, we also provide the results from the ensemble climate scenario where future crop yields are averages across five climate prediction models. We refer to this model as the "Ensemble Mean" in the following discussion.

Table 3 indicates that the impact of climate change on crop acreages and production within the MRB is mixed. Relative to the baseline with no climate change, corn acreage declines by 0.3% in CCSM4, and increases by 2.5% and 2.8% in the Ensemble Mean and IPSL-CM5A-LR, respectively. However, corn production decreases consistently in all models. Soybean acreage (production) decreases (increases) in future climates by 4.5% (5.8%) and 2.7% (5.0%) in the Ensemble Mean and IPSL-CM5A-LR, respectively. In the CCSM climate, soybean acreage increases by 0.3% and production decreases by 4.4%, respectively. Wheat acreage in future climates consistently declines relative to the baseline result. Changes in wheat production within the MRB are -4.6%, -0.9% and 5.0% under CCSM4, IPSL-CM5A-LR and the Ensemble Mean, respectively. Sorghum acreage and production decline in all models. Sorghum acreage (production) drops by 5.6% (8.3%), 16.7% (24.0%) and 5.6% (4.3%) in CCSM4, IPSL-CM5A-LR and the Ensemble Mean climates, respectively.

Changes in N use relative to the baseline are -0.8%, 2.2% and 1.9% in CCSM4, IPSL-CM5A-LR and the Ensemble Mean climate scenarios, respectively. Although changes in N use within the MRB are mixed across models, N delivered to the Gulf of Mexico consistently increases across all models (Table 3). Annual N runoff to the Gulf of Mexico increases compared to the baseline by 0.4% (CCSM4), 2.2% (IPSL-CM5A-LR) and 0.9% (Ensemble Mean). Although aggregate N use decreases in some models, N-intensive crop production shifts spatially to areas with high edge-of-field N leakage and Gulf runoff potential. As a result, cumulative N runoff to the Gulf increases in all models.

We also examine the implications of reducing N runoff to the Gulf by 45%

following EPA Hypoxia task force goal (Robertson and Saad, 2013) for consumer and producer surplus in each of the considered climate scenarios. We estimate the opportunity cost of reducing N runoff in terms of foregone consumer and producer surplus in the four considered commodity markets as N runoff externality is restricted. Last two rows of Table 3 show consumer and producer surplus values with and without the constraint limiting N runoff to the Gulf by 45%. The change in consumer and producer surplus estimates due to the N runoff constraint represents the opportunity cost of internalizing the N runoff externality (Xu et al., 2022). In the baseline scenario without climate change, consumer and producer surplus in the four commodity markets declines by $7.8 billion. This estimate varies between $6.3 and $8.1 billion depending on climate scenario. Hence, the opportunity cost of reducing the externality by 45% can increase by 3% (8.1/7.8) or decrease by 20% (6.3/7.8) depending on climate prediction models.

4.3 N runoff with altered precipitation in the MRB and crop yields outside the MRB

Next, we extend the preceding analysis by accounting for the effects of likely changes in precipitation within the MRB and changes in crop yields outside the MRB. We use predicted precipitation for future climate scenarios as a proxy for water availability in counties with irrigated agriculture within the MRB. We obtain 2050-2068 annual precipitation projections from GFDL-ESM2M-RegCM4, HadGEM2-ES-RegCM4 and MPI-ESM-LR-RegCM4 models provided by the National Center for Atmospheric Research (NCAR) (NCAR, 2022b).[3] We use these data to obtain mean annual precipitation across three models. Predicted changes in precipitation are combined with the baseline IHEAL water use solutions to generate

[3] RegCM4 (the Regional Climate Model version 4) is widely used to downscale global climate models for regional climate projections in the U.S. (Mei et al., 2013; Ashfaq et al., 2016). Our selection of global climate models for precipitation projection data is based on the availability of downscaled data in the NCAR database.

the county-scale water availability constraints for future climate change scenarios[4].

In this analysis, we also make an effort to account for the likely change in crop yields outside the MRB. Unfortunately, we do not have data on county specific effects of climate change on crop yields outside the MRB. Although land use outside the MRB is not critical for the purposes of this study, it is important to account for yield changes outside the MRB because of implications for national commodity supply and price. Therefore, we use the result from previous literature to adjust crop yields outside the MRB uniformly (Basche et al., 2016; Karimi et al., 2017; Chen et al., 2019). In particular, we assume that corn, soybean, wheat and sorghum yields outside of MRB will change by -1.6%, -2.7%, 7.0%, and -6.0%, respectively. We apply these adjustments to all models in Table 4.

Table 4 presents the aggregate MRB results from five climate models and the Ensemble Mean, including crop acreage and production, irrigated acreage, water use, N use and N delivery to the Gulf of Mexico. Values in parentheses are percentage changes relative to the baseline scenario in Table 3 (no climate change). We mainly discuss the Ensemble Mean model in this section. Ensemble Mean changes in corn, soybean and wheat acreages and production are consistent with the corresponding results in Table 3 in terms of signs and magnitudes. Ensemble Mean sorghum acreage within the MRB is the same in Tables 3 and 4. However, unlike Table 3, production increases in Table 4.

Changes in irrigated acreage and water use relative to the baseline scenario are consistent across Ensemble Mean solutions in Tables 3 and 4. However, Ensemble Mean irrigated acreage increases while water use declines within the MRB in Table 4 relative to Table 3. Two reasons explain this change. First, future precipitation is predicted to decline in counties located in Southern Kansas, Eastern New Mexico,

[4] Ensemble precipitation change is used for all climate model scenarios. A preferred approach would be to use precipitation change corresponding to each climate model used in IHEAL. Unfortunately, the precipitation prediction data for ACCESS1.3, MIROC5, IPSL-CM5A-LR, MIROC-ESM-CHEM and CCSM4 models are not available from the NCAR database.

Northern Texas, and Oklahoma, where agricultural production heavily relies on irrigation and precipitation. Water availability in these MRB counties decreases in Table 4 relative to Table 3, which leads to a reduction in total water use. Second, decrease in crop yields outside the MRB in Table 4 relative to Table 3 results in reallocation of some of the acreage from outside to inside the MRB. Hence, after adjusting water availability within the MRB and yields outside the MRB, acreage with irrigation increases, but total water use within the MRB declines in Table 4 relative to Table 3.

The Ensemble Mean N fertilizer use within the MRB is 30,000 metric tons lower in Table 4 than in Table 3. However, N runoff to the Gulf of Mexico is 490 metric tons greater in Table 4 than in Table 3. Two factors contribute to this divergence between N use and runoff in the Gulf of Mexico. First, within the MRB, corn, soybean and sorghum acreages increase by 0.05, 0.11 and 0.04 million ha, respectively, while wheat acreage decreases by 0.22 million ha. Cumulatively, the acreage of these crops decreases in Table 4 relative to Table 3, which leads to the modest decline in N use. Second, the increased corn, soybean and sorghum acreages occur in regions with both higher productivity and higher N runoff potential. As a result, N runoff to the Gulf of Mexico increases from crop production within the MRB. We explore the spatial distribution of N use and associated runoff to the Gulf in the next section.

Table 4 also shows estimates for consumer and producer surplus changes in the four commodity markets across climate scenarios and for the corresponding 45% N runoff reduction scenarios. Estimates for consumer and producer surplus do not change significantly relative to the corresponding estimates in table 3. All estimates of consumer and producer surplus without the N runoff reduction policy decline by less than one percent relative to table 3. Similar to the results in table 3, the opportunity cost of reducing N runoff by 45% varies between \$6.4 and \$8.3 billion.

4.4 Spatial distribution of N use and delivery to the Gulf of Mexico

The aggregate results show that in future climate scenarios, N delivery to the Gulf of Mexico from N fertilizer use within the MRB increases relative to the baseline. However, spatial heterogeneity is observed in terms of use and runoff contribution. In this section, the spatial distribution of N use (Figure 4) and the corresponding runoff (Figure 5) to the Gulf of Mexico is discussed, using the Ensemble Mean solutions in Table 4.

N use declines in Oklahoma, South Dakota and Texas, where corn yields in HAWQ-SWAT Ensemble Mean climate model decline by 10.8%, 13.3% and 3.2%, respectively. In these states, lower corn yields and greater demand for irrigation increase production costs, which leads to corn production shifting to other regions. Hence, N use in these regions declines (Figure 4). However, N use increases in some areas of Colorado, Western Kansas, Iowa, Illinois, Indiana, Minnesota, North Dakota, and Wisconsin. Although corn yields in these states also decrease, the higher marginal productivity of N fertilizer in these regions leads to more corn acreage and greater N use.

The largest increase in N use, from 11,903 to 17,000 metric tons per year, is observed in Tazewell County, IL. This growth in N use is due to the increase in corn and wheat acreages by 13,973 and 1,430 ha, respectively. Although corn yield in this county is predicted to decline by 8.5%, acreage increases as other counties suffer even greater yield losses and reduce corn production. The largest annual N use decrease from 10,087 to 1,700 metric tons is in Reno County, KS. This decrease is due to lower corn and wheat production as yields of these crops decline by 12.9% and 5.3%, respectively. In addition, precipitation in this county also declines by 0.1%.

Figure 5 presents county-specific changes in N delivery to the Gulf for the Ensemble Mean analysis relative to the baseline results. Agricultural production in the UMRB and OTRB delivers most of the N runoff to the Gulf of Mexico that originates in the MRB (Kling et al., 2014). These regions are currently targeted by the EPA's Hypoxia Task Force goals to reduce N runoff. The figure shows that N runoff from the UMRB may increase with climate change, while runoff from the OTRB may decrease relative to the baseline. States located in the UMRB, including Iowa, Illinois and Indiana, increase N delivery to the Gulf of Mexico relative to the baseline by 3,733 metric tons, a 1.4% increase. Increased N runoff from these states accounts for 99.3% of the predicted growth in N runoff to the Gulf. On the other hand, N runoff from Ohio, Tennessee and Kentucky (States located in OTRB) declines by 629 metric tons, a 2% reduction relative to the baseline runoff from these states.

5. Conclusion

This paper examines some of the effects of climate change on downstream water quality externality from agricultural production. Specifically, we investigate how climate-driven changes in crop yields affect agricultural production in the MRB and the corresponding water quality outcomes in the Gulf of Mexico. Our purpose is to illustrate, rather than predict, the potential impact of climate change on agricultural production externality in the form of N runoff to the Gulf. This dimension of the nexus between climate change and water resource sustainability has not received much attention in scientific literature. In this respect, our goal is to provide the first examination of its kind and spur additional research in this direction using integrated models with economic and biophysical components. The integrated approach is necessary because the behavioral response to environmental change is an important element of climate adaptation and can significantly affect downstream water quality.

This study differs from Metaxoglou and Smith in this volume in at least three important ways. First, we do not consider N legacy effects although it is an important part of Hypoxia in the Gulf of Mexico. Second, the IHEAL model includes N runoff from only four crops and excludes other crops and sectors including livestock and industrial production. Third, this study models N loads, while Metaxoglou and Smith investigate N concentrations. These differences imply that the results from the two studies cannot be directly compared.

We obtain three main findings. First, climate driven changes in crop yields affect agricultural production decisions in the MRB at intensive and extensive margins. Crop acreage and per acre N use are affected by changes in production conditions.

These changes increase the overall N delivery to the Gulf of Mexico from agricultural production, *ceteris paribus*. The estimated increase in N runoff to the Gulf is in the range of 0.5%-1.6% (1,690 -5,980 metric tons) relative to the baseline. These impacts are not substantial in terms of magnitude relative to current runoff. However, the corresponding marginal damages to aquatic ecosystems can be significant. Future studies should examine and evaluate the impacts of incremental increases in N runoff on Gulf aquatic ecosystems under climate change. Second, the changes in production, including N use, are spatially heterogeneous. In some counties, N use will intensify, while in others, N use will decrease. Third, spatial heterogeneity also applies at a larger spatial scale. As major contributors to the N runoff from agricultural production to the Gulf, the UMRB and OTRB are prioritized by the EPA's Hypoxia Task Force for reducing N runoff. In climate scenarios examined in this study, N runoff is expected to increase from the UMRB and decrease from the OTRB.

We also examine the sensitivity of the opportunity costs to reduce N runoff to the Gulf by 45% across climate scenarios. The results show that without climate change, the opportunity cost is $7.8 billion while with climate change this estimate varies between $6.4 and $8.1 billion. Our N runoff reduction scenario is akin to a performance-based policy where internalizing the N runoff externality reduces N runoff by 45%. Although not directly addressed in this study, an example of a performance-based policy is tradeable pollution permit system that imposes an exogenous upper bound on environmental impact. With frictionless trade in the permits market, cost-effective distribution of production and mitigation efforts can be achieved under various emissions caps (Montgomery, 1972; Cropper and Oates, 1992). Cap and trade policies are operationally and politically challenging to implement even if technologically feasible. Nevertheless, while a detailed examination of tradable permit-based runoff mitigation is beyond the scope of this study, our results are informative in terms providing an estimate for the opportunity cost of such a policy in the four commodity markets and in terms of examining the sensitivity of the estimated costs across several climate models.

Several limitations of this study should be mentioned for future research. First, climate change can affect not only crop yields but also water balance. In some regions, changes in climate can influence soil water properties and surface and groundwater interactions (Scibek et al., 2007; Saha et al., 2017; Guevara-Ochoa et al., 2020). In this study, we do not account for ground versus surface water availability explicitly. Instead, precipitation changes, as predicted by the climate models included in this study and reported in the NCAR database, are used to examine the impact of changes in water availability. The explicit delineation between ground and surface water irrigation, and the associated impacts of climate change, will improve the accuracy of our estimates.

Second, the modeling exercise does not account for potential changes in the edge-of-field N runoff and N delivery ratios from cropland to the Gulf in future climate scenarios. This may over or underestimate N loading in the Gulf of Mexico. Unfortunately, estimates of climate impact on spatial and temporal attributes of N delivery ratios to the Gulf have not been produced yet.

Third, crop yield changes under future climates outside the MRB are assumed to be uniform across all counties. The assumed uniformity in yield change outside the MRB precludes the analysis of impacts on N runoff outside the MRB but is less critical for the purpose of this paper. We use these uniform yield changes outside the MRB to account for the potential effect on national commodity supply and prices which can influence production decisions within the MRB and associated N runoff. More detailed modeling of yield changes in areas outside the MRB may improve the accuracy of our estimates and enable analysis of N impacts outside of the MRB.

Fourth, we do not explicitly account for the effect of precipitation change in non-irrigated regions. Instead, we assume that precipitation affects water availability only in the areas with non-zero irrigation, as observed in the past data because irrigation water availability depends at least in part on precipitation. In addition, we do not explicitly account for irrigation infrastructure that links precipitation and irrigation water supply. For non-irrigated regions, we do not have estimates for the effect of precipitation or irrigation on crop yields. This is an important caveat that should be addressed in future studies. A decline in precipitation in rainfed crop production regions may prompt investment in irrigation infrastructure, which we do not include in the current study. Conversely, we also do not account for potential increase in precipitation or flooding effects in non-irrigated regions that can influence production decisions and N delivery ratios.

Fifth, the IHEAL model corresponds to the social planner's problem with perfect information. Crop production, land and input use (N and water) are obtained based on social welfare maximization. This framework is consistent with Potential Pareto Optimality criteria but does not explicitly consider implications for strict Pareto Optimality (Griffin, 1995). Nevertheless, in terms of long run equilibrium outcomes, the model provides useful insights for illustrating the potential impacts of agricultural production on downstream water quality. Such models have been extensively used for various policy-relevant analyses (Havlik et al., 2011; Chen et al., 2014; Xu et al., 2022).

Despite the limitations, the study provides a useful initial evaluation of the impacts of agricultural production adaptation to climate change on downstream water quality. Our purpose in this study is not to predict the water quality outcomes. Instead, our purpose is to draw attention to a previously unaddressed climate related issue, which is the externality of agricultural production adaptation to climate change in terms of nutrient runoff and downstream water quality. The initial estimates in this study show that N runoff can increase by 0.5%-1.6% (1,690 -5,980 metric tons), and reducing N runoff by 45% will be from 18.0% less to 6.4% more costly depending on climate change scenario relative to the baseline. We do not claim to have addressed this issue comprehensively, but the results suggest that future studies should examine the nutrient runoff externalities from agricultural production adaptation to climate change in greater detail.

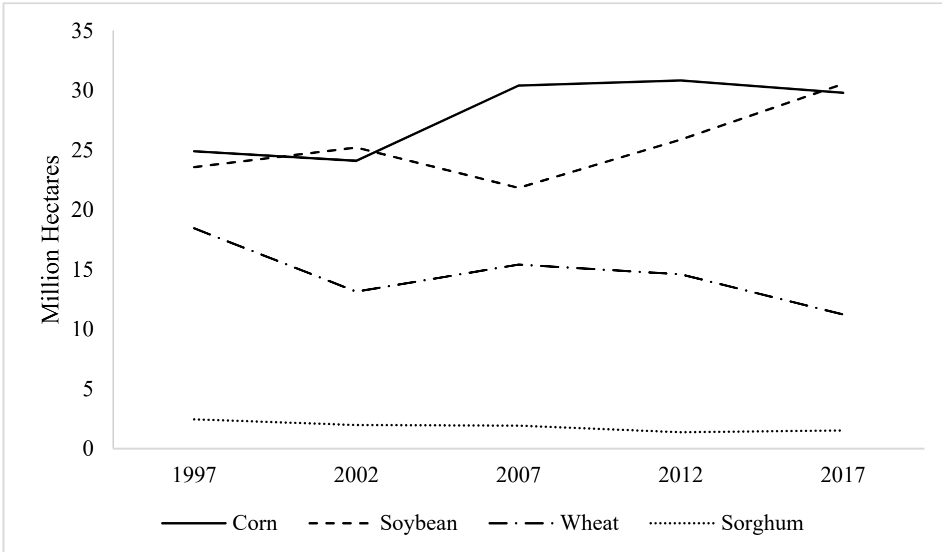

Figure 1. Harvested acreage within the MRB over time (ha)

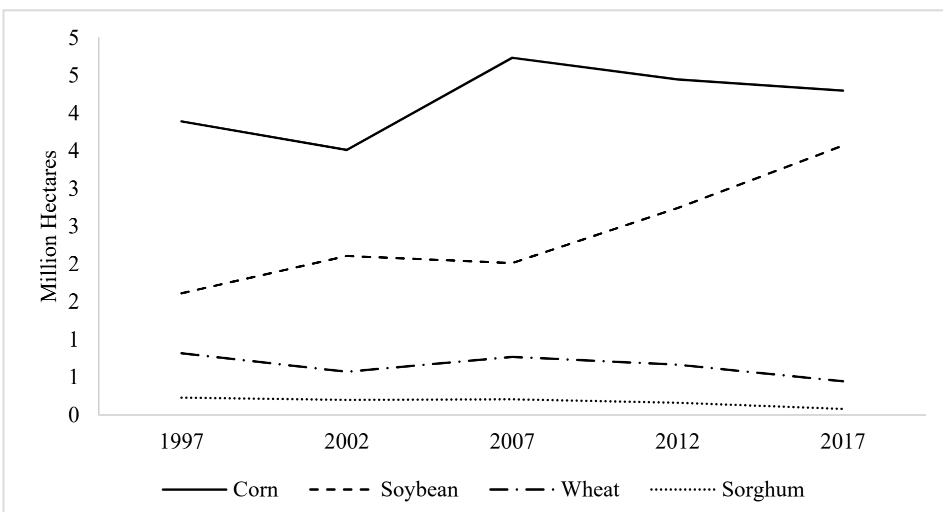

Figure 2. Harvested irrigated acreage within the MRB over time (ha)

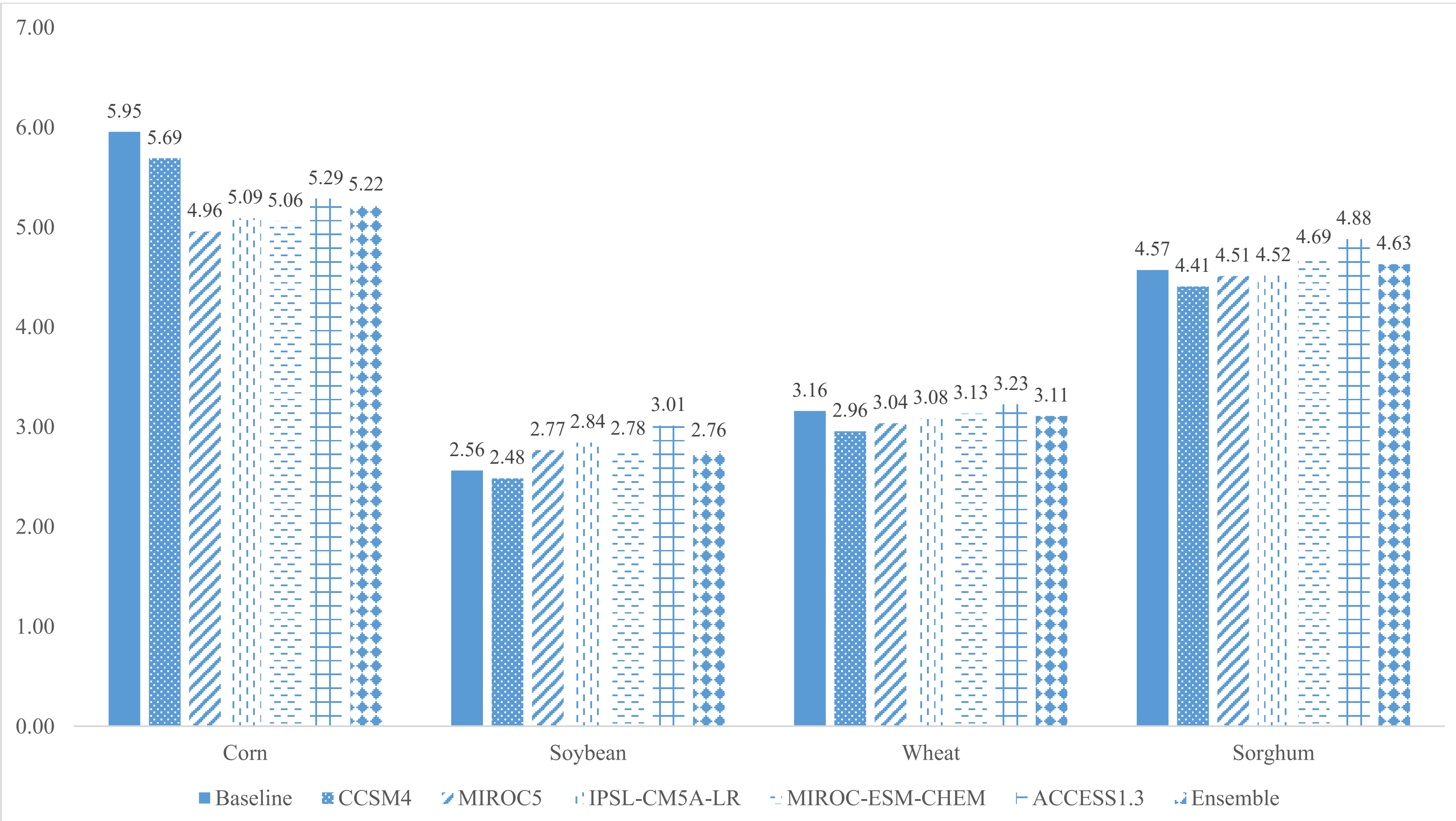

Figure 3. The mean of crop yields under historical and future climates over all counties within the MRB (t/ha)

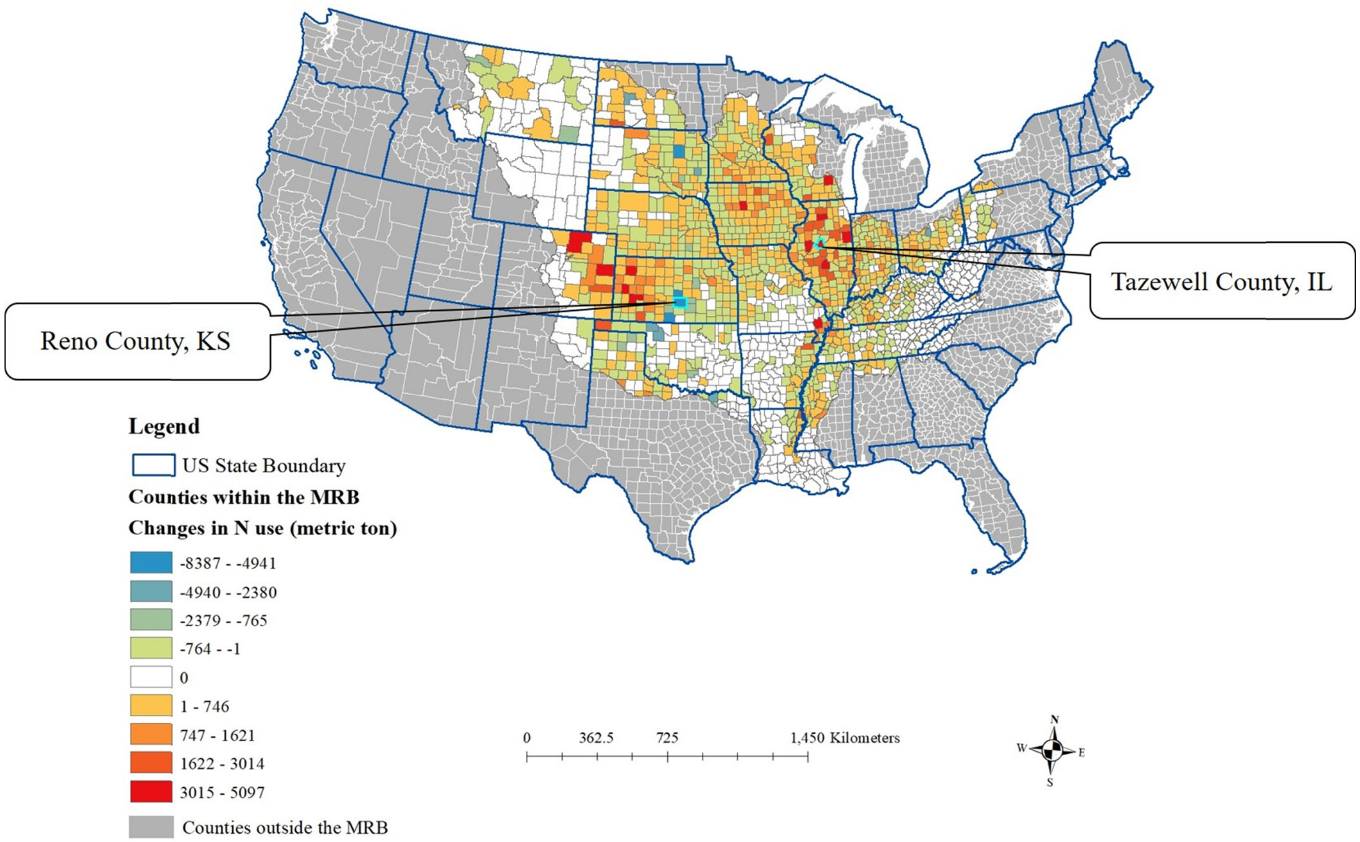

Figure 4. Spatial distribution of N use in the Ensemble Mean of Table 4

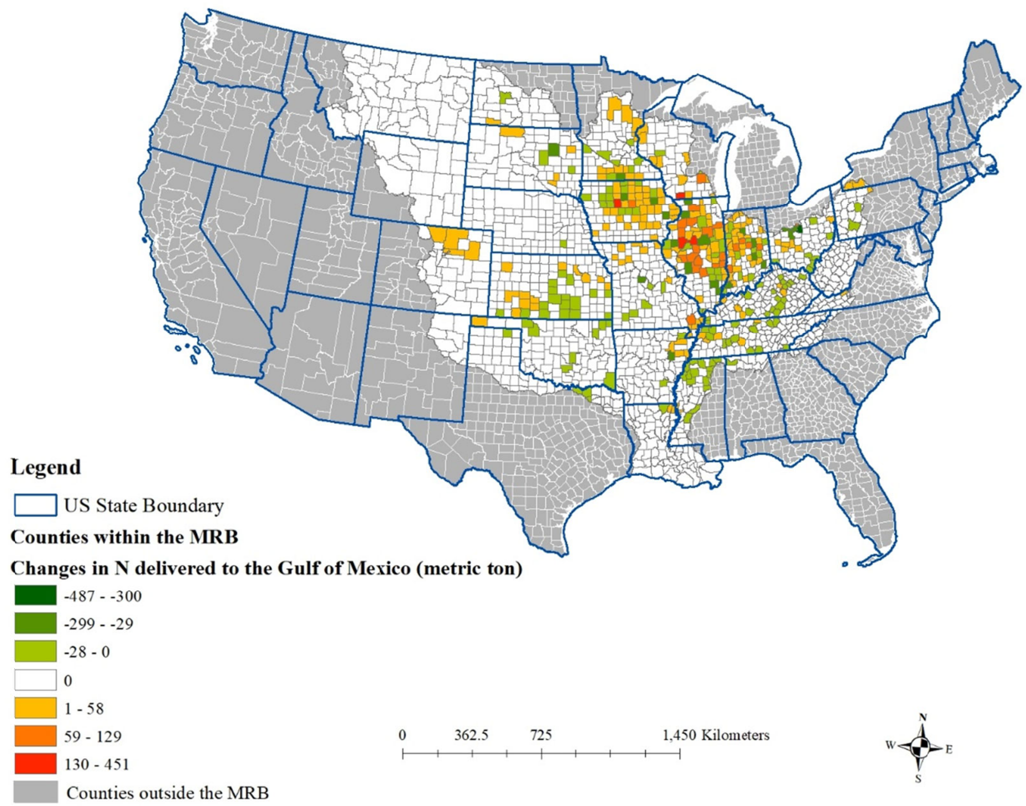

Figure 5. Spatial distribution of N delivered to the Gulf of Mexico in the Ensemble Mean of Table 4

Table 1. List of climate models used in this study[a]

Model	Institution	Resolution
Access1.3	CSIRO-BOM (Australia)	1.875*1.25
CCSM	NCAR (USA)	0.9*1.25
IPSL-CM5A-LR	IPSL (France)	1.875*3.75
MIROC-ESM-CHEM	MIROC (Japan)	2.8*2.8
MIROC5	MIROC (Japan)	2.8*2.8

[a] Source: Harding et al. (2013)

Table 2. Validation and baseline results

	Validation results (historical crop mix)	Observed in 2018[ab]	Baseline results (historical and synthetic crop mix)
	LAND USE (MILLION HECTARES) FOR THE CONTIGUOUS UNITED STATES		
Corn	39.6	36.0	38.2
Soybean	39.1	36.1	37.6
Winter wheat	14.5	13.2	12.4
Sorghum	2.4	2.3	2.2
	PRICES ($/METRIC TON)		
Corn Price	140.6	142	147.7
Soybean Price	312.6	314	335.4
Wheat Price	182.3	190	216.0
Sorghum Price	119.0	117	133.5

	Validation results (historical crop mix)	Values from literature	Baseline results (historical and synthetic crop mix)
Total irrigated acreage (million ha)	3.92 (MRB)	7.49 (MRB)[c]	3.96 (MRB)
Total water use (million acre-feet)	4.52 (MRB)	83.40 (U.S.)[a]	4.57 (MRB)
N applied within the MRB (1000 metric ton)	6,835 (MRB)	12,610 (U.S.)[d]	6,798 (MRB)
N delivered to the Gulf of Mexico from fertilizer application (metric ton)	370,140 (MRB)	796,000 (MRB)[ef]	369,190 (MRB)

[a] Source: USDA NASS, 2019
[b] Baseline model data, including prices and quantities for commodity demands are from 2018. Hence, we compare the baseline results with data observed in 2018.
[c] Total irrigated acreage of corn, soybean wheat and sorghum in the MRB in 2018 were 7,489,765 ha (USDA NASS, 2019).
[d] The sum of county-level farm N fertilizer use (Falcone, 2021).
[e] Source: White et al., 2014.
[f] N fertilizer use in crop production accounts for 68% of N delivered to the Gulf of Mexico from agriculture. The rest of N exported to the Gulf from agriculture comes from confined animal operations and legume crops (USGS, 2017).

Table 3. Results under future climates

	Baseline	Ensemble Mean	CCSM4	ACCESS1.3	IPSL-CM5A-LR	MIROC-ESM-CHEM	MIROC5
Corn acreage within the MRB (million ha)	31.6	32.5	31.5	32.8	32.4	32.8	32.5
Corn production within the MRB (million metric ton)	320.3	294.4	308.4	307.6	280.4	280.1	276.8
Soybean acreage within the MRB (million ha)	29.1	28.3	29.2	27.3	27.8	28.1	28
Soybean production within the MRB (million metric ton)	98.4	103.3	94	111.9	104.1	102	101.7
Wheat acreage within the MRB (million ha)	9.4	9.1	9.2	8.8	9.2	9.4	8.8
Wheat production within the MRB (million metric ton)	21.9	23.0	20.9	25.5	21.7	24.8	22.6
Sorghum acreage within the MRB (million ha)	1.8	1.7	1.7	1.7	1.5	1.6	1.6
Sorghum production within the MRB (million metric ton)	7.6	7.3	7	8.4	5.8	6.5	6.5
Irrigated Acreage within the MRB (ha)	3,955,607	3,979,146	3,934,678	3,953,137	3,919,521	3,922,389	3,916,433
Total water use within the MRB (million acre-feet)	4.57	4.11	4.5	4.16	4.62	4.69	4.07
N applied within the MRB (1000 metric ton)	6,798	6,930	6,747	6,931	6,948	7,006	6,874
N delivered to the Gulf of Mexico from fertilizer application (metric ton)	369,190	372,410	370,650	370,990	375,010	373,310	372,940
Consumer and producer surplus for four commodities (billion $)	204.8	202.1	201.3	207.7	199.8	199.2	198.6
Consumer and producer surplus with a 45% N runoff reduction from MRB relative to the baseline (billion $)	197.0	194.9	193.2	201.4	192.1	192.3	191.1

Table 4. Results with changes in water availability and crop yields adjusted outside the MRB under future climates

	Ensemble Mean	CCSM4	ACCESS1.3	IPSL-CM5A-LR	MIROC-ESM-CHEM	MIROC5
Corn acreage within the MRB (million ha)	32.6 (3.2%)	31.5 (-0.3%)	32.8 (3.8%)	32.5 (2.8%)	32.9 (4.1%)	32.6 (3.2%)
Corn production within the MRB (million metric ton)	294.4 (-8.1%)	308.6 (-3.7%)	307.6 (-4.0%)	280.8 (-12.3%)	280.2 (-12.5%)	277.1 (-13.5%)
Soybean acreage within the MRB (million ha)	28.4 (-2.4%)	29.2 (0.3%)	27.4 (-5.8%)	27.8 (-4.5%)	28.1 (-3.4%)	28.1 (-3.4%)
Soybean production within the MRB (million metric ton)	103.6 (5.3%)	94.1 (-4.4%)	112.2 (14.0%)	104.2 (5.9%)	102.2 (3.9%)	101.9 (3.6%)
Wheat acreage within the MRB (million ha)	8.9 (-5.3%)	8.8 (-6.4%)	8.6 (-8.5%)	8.8 (-6.4%)	8.9 (-5.3%)	8.6 (-8.5%)
Wheat production within the MRB (million metric ton)	22.4 (2.3%)	20.0 (-8.7%)	24.8 (13.2%)	20.9 (-4.6%)	23.6 (7.8%)	22.1 (0.9%)
Sorghum acreage within the MRB (million ha)	1.7 (-5.6%)	1.7 (-5.6%)	1.7 (-5.6%)	1.6 (-11.1%)	1.6 (-11.1%)	1.6 (-11.1%)
Sorghum production within the MRB (million metric ton)	7.7 (0.9%)	7.4 (-3.0%)	8.4 (10.1%)	6.5 (-14.8%)	6.7 (-12.2%)	6.8 (-10.9%)
Irrigated Acreage within the MRB (ha)	3,990,864 (0.9%)	3,949,977 (-0.1%)	3,933,342 (-0.6%)	3,937,504 (-0.5%)	3,927,531 (-0.7%)	3,922,191 (-0.8%)
Total water use within the MRB (million acre-feet)	3.91 (-14.4%)	4.45 (-2.6%)	3.90 (14.7%)	4.41 (-3.5%)	4.37 (-4.4%)	3.80 (-16.8%)
N applied within the MRB (1000 metric ton)	6,915 (1.7%)	6,720 (-1.1%)	6,912 (1.7%)	6,927 (1.9%)	6,971 (2.5%)	6,871 (1.1%)
N delivered to the Gulf of Mexico from fertilizer application (metric ton)	372,900 (1.0%)	370,880 (0.5%)	371,420 (0.6%)	375,170 (1.6%)	373,480 (1.2%)	373,050 (1.0%)
Consumer and producer surplus for four commodities (billion $)	201.9	201.1	207.5	199.6	199.0	198.4
Consumer and producer surplus with a 45% N runoff reduction from MRB relative to the baseline (billion $)	194.5	192.8	201.1	191.7	191.9	190.7

Reference

Ashfaq, M., Rastogi, D., Mei, R., Kao, S.C., Gangrade, S., Naz, B.S. and Touma, D., 2016. High-resolution ensemble projections of near-term regional climate over the continental United States. Journal of Geophysical Research: Atmospheres, 121(17), pp.9943-9963.

Basche, A.D., Archontoulis, S.V., Kaspar, T.C., Jaynes, D.B., Parkin, T.B. and Miguez, F.E., 2016. Simulating long-term impacts of cover crops and climate change on crop production and environmental outcomes in the Midwestern United States. Agriculture, Ecosystems & Environment, 218, pp.95-106.

Bosch, D.J., Wagena, M.B., Ross, A.C., Collick, A.S. and Easton, Z.M., 2018. Meeting water quality goals under climate change in Chesapeake Bay watershed, USA. JAWRA Journal of the American Water Resources Association, 54(6), pp.1239-1257.

Chen, X. and Önal, H., 2012. Modeling agricultural supply response using mathematical programming and crop mixes. American Journal of Agricultural Economics, 94(3), pp.674-686.

Chen, X., Huang, H., Khanna, M. and Önal, H., 2014. Alternative transportation fuel standards: Welfare effects and climate benefits. Journal of Environmental Economics and Management, 67(3), pp.241-257.

Chen, Y., Marek, G.W., Marek, T.H., Moorhead, J.E., Heflin, K.R., Brauer, D.K., Gowda, P.H. and Srinivasan, R., 2019. Simulating the impacts of climate change on hydrology and crop production in the Northern High Plains of Texas using an improved SWAT model. Agricultural Water Management, 221, pp.13-24.

Cropper, M.L. and Oates, W.E., 1992. Environmental economics: a survey. Journal of economic literature, 30(2), pp.675-740.

Dieter, C.A., Linsey, K.S., Caldwell, R.R., Harris, M.A., Ivahnenko, T.I., Lovelace, J.K., Maupin, M.A. and Barber, N.L., 2018. Estimated use of water in the United States county-level data for 2015 (ver. 2.0, June 2018). US Geological Survey data release, 10, p.F7TB15V5.

Griffin, R.C., 1995. On the meaning of economic efficiency in policy analysis. Land Economics, pp.1-15.

Guevara-Ochoa, C., Medina-Sierra, A. and Vives, L., 2020. Spatio-temporal effect of climate change on water balance and interactions between groundwater and surface water in plains. Science of the Total Environment, 722, p.137886.

Harding, K.J., Snyder, P.K. and Liess, S., 2013. Use of dynamical downscaling to improve the simulation of Central US warm season precipitation in CMIP5 models. Journal of Geophysical Research: Atmospheres, 118(22), pp.12-522.

HAWQS, 2020, "HAWQS System and Data to model the lower 48 conterminous U.S using the SWAT model", https://doi.org/10.18738/T8/XN3TE0, Texas Data Repository Dataverse, V1

Havlík, P., Schneider, U.A., Schmid, E., Böttcher, H., Fritz, S., Skalský, R., Aoki, K., De Cara, S., Kindermann, G., Kraxner, F. and Leduc, S., 2011. Global land-use implications of first and second generation biofuel targets. Energy policy, 39(10), pp.5690-5702.

Ishida, K. and Jaime, M., 2015. A Partial Equilibrium of the Sorghum Markets in US, Mexico, and Japan (No. 330-2016-13894, pp. 1-1).

Karimi, T., Stöckle, C.O., Higgins, S.S., Nelson, R.L. and Huggins, D., 2017. Projected dryland cropping system shifts in the Pacific Northwest in response to climate change. Frontiers in Ecology and Evolution, 5, p.20.

Kling, C.L., Panagopoulos, Y., Rabotyagov, S.S., Valcu, A.M., Gassman, P.W., Campbell, T., White, M.J., Arnold, J.G., Srinivasan, R., Jha, M.K. and Richardson, J.J., 2014. LUMINATE: linking agricultural land use, local water quality and Gulf of Mexico hypoxia. European Review of Agricultural Economics, 41(3), pp.431-459.

Kumar, S. and Merwade, V., 2011. Evaluation of NARR and CLM3. 5 outputs for surface water and energy budgets in the Mississippi River Basin. Journal of Geophysical Research: Atmospheres, 116(D8).

Marshall, K. K., Riche, S. M., Seeley, R. M., Westcott, P. C. 2015. Effects of recent energy price reductions on US agriculture. United States Department of Agriculture, Economic Research Service.

Marshall, E., Aillery, M., Ribaudo, M., Key, N., Sneeringer, S., Hansen, L., Malcolm, S. and Riddle, A., 2018. Reducing nutrient losses from cropland in the Mississippi/Atchafalaya River Basin: Cost efficiency and regional distribution (No. 1477-2018-5724).

Montgomery, W.D., 1972. Markets in licenses and efficient pollution control programs. Journal of economic theory, 5(3), pp.395-418.

Mei, R., Wang, G. and Gu, H., 2013. Summer land–atmosphere coupling strength over the United States: Results from the regional climate model RegCM4–CLM3. 5. Journal of Hydrometeorology, 14(3), pp.946-962.

National Center for Atmospheric Research (NCAR). 2022a. North American Regional Climate Change Assessment Program. Available at: https://www.narccap.ucar.edu/results/index.html#climate-change. (Accessed on March 10, 2022)

NCAR. 2022b. Climate Data Gateway at NCAR. Available at: https://www.earthsystemgrid.org/. (Accessed on March 10, 2022)

Panagopoulos, Y., Gassman, P.W., Arritt, R.W., Herzmann, D.E., Campbell, T.D., Jha, M.K., Kling, C.L., Srinivasan, R., White, M. and Arnold, J.G., 2014. Surface water quality and cropping systems sustainability under a changing climate in the Upper Mississippi River Basin. Journal of Soil and Water Conservation, 69(6), pp.483-494.

Panagopoulos, Y., Gassman, P.W., Arritt, R.W., Herzmann, D.E., Campbell, T.D., Valcu, A., Jha, M.K., Kling, C.L., Srinivasan, R., White, M. and Arnold, J.G., 2015. Impacts of climate change on hydrology, water quality and crop productivity in the Ohio-Tennessee River Basin. International Journal of Agricultural and Biological Engineering, 8(3), pp.36-53.

Piggott, N.E. and Wohlgenant, M.K., 2002. Price elasticities, joint products, and international trade. Australian Journal of Agricultural and Resource Economics, 46(4), pp.487-500.

Robertson, D.M. and Saad, D.A., 2013. SPARROW models used to understand nutrient sources in the Mississippi/Atchafalaya River Basin. Journal of Environmental Quality, 42(5), pp.1422-1440.

Saha, G.C., Li, J., Thring, R.W., Hirshfield, F. and Paul, S.S., 2017. Temporal dynamics of groundwater-surface water interaction under the effects of climate change: a case study in the Kiskatinaw River Watershed, Canada. Journal of Hydrology, 551, pp.440-452.

Scibek, J., Allen, D.M., Cannon, A.J. and Whitfield, P.H., 2007. Groundwater–surface water interaction under scenarios of climate change using a high-resolution transient groundwater model. Journal of Hydrology, 333(2-4), pp.165-181.

Smit, B. and Skinner, M.W., 2002. Adaptation options in agriculture to climate change: a typology. Mitigation and adaptation strategies for global change, 7(1), pp.85-114.

Steiner, J.L., Devlin, D.L., Perkins, S., Aguilar, J.P., Golden, B., Santos, E.A. and Unruh, M., 2021. Policy, Technology, and Management Options for Water Conservation in the Ogallala Aquifer in Kansas, USA. Water, 13(23), p.3406.

U.S. Environmental Protection Agency (US EPA). 2014. Mississippi River Gulf of Mexico Watershed Nutrient Task Force New Goal Framework. https://www.epa.gov/sites/production/files/2015-07/documents/htf-goals-framework-2015.pdf. (Accessed on Dec 2021)

US EPA. 2019. Hypoxia 101. https://www.epa.gov/ms-htf/hypoxia-101. (Accessed on Dec 2021)

US EPA. 2021a. Northern Gulf of Mexico Hypoxic Zone. Available at: https://www.epa.gov/ms-htf/northern-gulf-mexico-hypoxic-zone. (Accessed on Dec 2021)

US EPA. 2021b. Hypoxia Task Force Nutrient Reduction Strategies. Available at: https://www.epa.gov/ms-htf/hypoxia-task-force-nutrient-reduction-strategies. (Accessed on Dec 2021)

USDA ERS (United States Department of Agriculture Economic Research Service). 2019. Fertilizer Use and Price. https://www.ers.usda.gov/data-products/fertilizer-use-and-price. (accessed 30 Oct 2019).

USDA ERS. 2021. Irrigation & Water Use. Available at: https://www.ers.usda.gov/topics/farm-practices-management/irrigation-water-use/. (Accessed on Dec 2021)

USDA ERS. 2022. Irrigated cropping patterns in the United States have evolved significantly since 1964. Available at: https://www.ers.usda.gov/data-products/chart-gallery/gallery/chart-detail/?chartId=103568. (Accessed on July 2022)

U.S. Department of Agriculture National Agricultural Statistics Service (USDA NASS). 2019. 2017 Census of Agriculture. Available at: www.nass.usda.gov/AgCensus. (Accessed on Dec 2021)

USDA NASS. 2020. U.S. &All States County Data – Crops. Washington, DC. http://www.nass.usda.gov/. (accessed 13 May 2021).

U.S. Geological Survey (USGS). 2018. Water-use data available from USGS. https://water.usgs.gov/watuse/data/index.html. (accessed 1 Jan 2022).

Westcott, P.C. and Hoffman, L.A., 1999. Price determination for corn and wheat: the role of market factors and government programs (No. 1488-2016-123383).

White, M.J., Santhi, C., Kannan, N., Arnold, J.G., Harmel, D., Norfleet, L., Allen, P., DiLuzio, M., Wang, X., Atwood, J. and Haney, E., 2014. Nutrient delivery from the Mississippi River to the Gulf of Mexico and effects of cropland conservation. Journal of Soil and Water Conservation, 69(1), pp.26-40.

Wu, D., Qu, J.J. and Hao, X., 2015. Agricultural drought monitoring using MODIS-based drought indices over the USA Corn Belt. International Journal of Remote Sensing, 36(21), pp.5403-5425.

Xu, Y., Bosch, D.J., Wagena, M.B., Collick, A.S. and Easton, Z.M., 2019. Meeting water quality goals by spatial targeting of best management practices under climate change. Environmental management, 63(2), pp.173-184.

Xu, Y., Elbakidze, L., Yen, H., Arnold, J.G., Gassman, P.W., Hubbart, J. and Strager, M.P., 2022. Integrated assessment of nitrogen runoff to the Gulf of Mexico. Resource and Energy Economics, 67, p.101279.

Appendix

$$\max_{x,n_1,n_2,w_1} \pi = \int_0^{\mathrm{x}} \mathrm{p}(t)\,dt - C_n * (n_1 + n_2) - C_w * w_1 \text{ (S1)}$$

subject to

$$\alpha_1 * f(n_1, w_1) + \alpha_2 * g(n_2) \geq \mathrm{x} \ (S2)$$

Lagrangian and corresponding first order conditions are as follows:

$$\mathrm{L} = \int_0^{\mathrm{x}} \mathrm{p}(t)\,dt - C_n * (n_1 + n_2) - C_w * w_1 + \lambda(\alpha_1 * f(n_1, w_1) + \alpha_2 * g(n_2) - \mathrm{x}) \text{ (S3)}$$

$[x]$ $\quad \frac{\partial L}{\partial x} = \mathrm{p(x)} - \lambda = 0 \quad \text{(S4)}$

$[n_1]$ $\quad \frac{\partial L}{\partial n_1} = -C_n + \lambda \alpha_1 f_{n_1} = 0$

$[n_2]$ $\quad \frac{\partial L}{\partial n_2} = -C_n + \lambda \alpha_2 g_{n_2} = 0$

$[w_1]$ $\quad \frac{\partial L}{\partial w_1} = -C_w + \lambda \alpha_1 f_{w_1} = 0$

$[\lambda]$ $\quad \frac{\partial L}{\partial \lambda} = \alpha_1 * f(n_1, w_1) + \alpha_2 * g(n_2) - \mathrm{x} = 0$

Total differentiation of the first order conditions with respect to α_1 gives:

$[x]$ $\quad p_{\mathrm{x}} \frac{\partial \mathrm{x}}{\partial \alpha_1} - \frac{\partial \lambda}{\partial \alpha_1} = 0 \quad \text{(S5)}$

$[n_1]$ $\quad \lambda \alpha_1 f_{n_1 n_1} \frac{\partial n_1}{\partial \alpha_1} + \lambda \alpha_1 f_{n_1 w_1} \frac{\partial w_1}{\partial \alpha_1} + \alpha_1 f_{n_1} \frac{\partial \lambda}{\partial \alpha_1} = -\lambda f_{n_1}$

$$[n_2] \qquad \lambda\alpha_2 g_{n_2n_2}\frac{\partial n_2}{\partial\alpha_1}+\alpha_2 g_{n_2}\frac{\partial\lambda}{\partial\alpha_1}=0$$

$$[w_1] \quad \lambda\alpha_1 f_{w_1n_1}\frac{\partial n_1}{\partial\alpha_1}+\lambda\alpha_1 f_{w_1w_1}\frac{\partial w_1}{\partial\alpha_1}+\alpha_1 f_{w_1}\frac{\partial\lambda}{\partial\alpha_1}=-\lambda f_{w_1}$$

$$[\lambda] \quad \alpha_1 f_{n_1}\frac{\partial n_1}{\partial\alpha_1}+\alpha_1 f_{w_1}\frac{\partial w_1}{\partial\alpha_1}+\alpha_2 g_{n_2}\frac{\partial n_2}{\partial\alpha_1}-\frac{\partial x}{\partial\alpha_1}=-f(n_1,w_1)$$

The second order conditions can be expressed in terms of the Bordered Hessian representation as $AH = B$, where $A=\left[\frac{\partial x}{\partial\alpha_1},\frac{\partial n_1}{\partial\alpha_1},\frac{\partial n_2}{\partial\alpha_1},\frac{\partial w_1}{\partial\alpha_1},\frac{\partial\lambda}{\partial\alpha_1}\right]$ is the vector of derivatives of all endogenous variables w.r.t τ. H is the Hessian matrix shown below, and $B=\left[0,-\lambda f_{n_1},0,-\lambda f_{w_1},-f(n_1,w_1)\right]$.

$$H=\begin{bmatrix} p_x & 0 & 0 & 0 & -1 \\ 0 & \lambda\alpha_1 f_{n_1n_1} & 0 & \lambda\alpha_1 f_{w_1n_1} & \alpha_1 f_{n_1} \\ 0 & 0 & \lambda\alpha_2 g_{n_2n_2} & 0 & \alpha_2 g_{n_2} \\ 0 & \lambda\alpha_1 f_{n_1w_1} & 0 & \lambda\alpha_1 f_{w_1w_1} & \alpha_1 f_{w_1} \\ -1 & \alpha_1 f_{n_1} & \alpha_2 g_{n_2} & \alpha_1 f_{w_1} & 0 \end{bmatrix} \quad (S6)$$

$$|H| = \alpha_1^2\alpha_2\lambda^2\Big[2\alpha_1 f_{n_1} f_{n_1w_1} f_{w_1} g_{n_2n_2} p_x - \alpha_1 f_{n_1}^2 f_{w_1w_1} g_{n_2n_2} p_x + f_{n_1w_1}^2\left(\lambda g_{n_2n_2}+\alpha_2 p_x g_{n_2}^2\right) - f_{n_1n_1}\left(\lambda f_{w_1w_1} g_{n_2n_2} + \alpha_2 f_{w_1w_1} p_x g_{n_2}^2 + \alpha_1 f_{w_1}^2 g_{n_2n_2} p_x\right)\Big] \quad (S7)$$

$$\frac{\partial n_1}{\partial\alpha_1}=\frac{|H_{n_1}|}{|H|}$$

$$=\frac{-\alpha_1\alpha_2\lambda^2\left(f_{n_1w_1}f_{w_1}-f_{n_1}f_{w_1w_1}\right)\left(\alpha_2 p_x g_{n_2}^2+g_{n_2n_2}\left(\lambda+\alpha_1 p_x f(n_1,w_1)\right)\right)}{\alpha_1^2\alpha_2\lambda^2\left[2\alpha_1 f_{n_1}f_{n_1w_1}f_{w_1}g_{n_2n_2}p_x-\alpha_1 f_{n_1}^2 f_{w_1w_1}g_{n_2n_2}p_x+f_{n_1w_1}^2\left(\lambda g_{n_2n_2}+\alpha_2 p_x g_{n_2}^2\right)-f_{n_1n_1}\left(\lambda f_{w_1w_1}g_{n_2n_2}+\alpha_2 f_{w_1w_1}p_x g_{n_2}^2+\alpha_1 f_{w_1}^2 g_{n_2n_2}p_x\right)\right]}$$

$$=\frac{-\left(f_{n_1w_1}f_{w_1}-f_{n_1}f_{w_1w_1}\right)\left(\alpha_2 p_x g_{n_2}^2+g_{n_2n_2}\left(\lambda+\alpha_1 p_x f(n_1,w_1)\right)\right)}{\alpha_1\left[2\alpha_1 f_{n_1}f_{n_1w_1}f_{w_1}g_{n_2n_2}p_x-\alpha_1 f_{n_1}^2 f_{w_1w_1}g_{n_2n_2}p_x+f_{n_1w_1}^2\left(\lambda g_{n_2n_2}+\alpha_2 p_x g_{n_2}^2\right)-f_{n_1n_1}\left(\lambda f_{w_1w_1}g_{n_2n_2}+\alpha_2 f_{w_1w_1}p_x g_{n_2}^2+\alpha_1 f_{w_1}^2 g_{n_2n_2}p_x\right)\right]} \quad (S8)$$

$$\frac{\partial n_2}{\partial \alpha_1} = \frac{|H_{n_2}|}{|H|}$$

$$= \frac{-\alpha_1{}^2\alpha_2\lambda^2 g_{n_2} p_{\mathrm{x}} \left[-2f_{n_1}f_{n_1w_1}f_{w_1} + f_{n_1n_1}f_{w_1}{}^2 + f(n_1,w_1)\left(f_{n_1w_1}{}^2 - f_{n_1n_1}f_{w_1w_1}\right)\right]}{\alpha_1{}^2\alpha_2\lambda^2\left[2\alpha_1 f_{n_1}f_{n_1w_1}f_{w_1}g_{n_2n_2}p_x - \alpha_1 f_{n_1}{}^2 f_{w_1w_1}g_{n_2n_2}p_x + f_{n_1w_1}{}^2\left(\lambda g_{n_2n_2} + \alpha_2 p_{\mathrm{x}} g_{n_2}{}^2\right) - f_{n_1n_1}\left(\lambda f_{w_1w_1}g_{n_2n_2} + \alpha_2 f_{w_1w_1}p_{\mathrm{x}}g_{n_2}{}^2 + \alpha_1 f_{w_1}{}^2 g_{n_2n_2}p_x\right)\right]}$$

$$= \frac{-g_{n_2} p_{\mathrm{x}} \left[-2f_{n_1}f_{n_1w_1}f_{w_1} + f_{n_1n_1}f_{w_1}{}^2 + f(n_1,w_1)\left(f_{n_1w_1}{}^2 - f_{n_1n_1}f_{w_1w_1}\right)\right]}{2\alpha_1 f_{n_1}f_{n_1w_1}f_{w_1}g_{n_2n_2}p_x - \alpha_1 f_{n_1}{}^2 f_{w_1w_1}g_{n_2n_2}p_x + f_{n_1w_1}{}^2\left(\lambda g_{n_2n_2} + \alpha_2 p_{\mathrm{x}} g_{n_2}{}^2\right) - f_{n_1n_1}\left(\lambda f_{w_1w_1}g_{n_2n_2} + \alpha_2 f_{w_1w_1}p_{\mathrm{x}}g_{n_2}{}^2 + \alpha_1 f_{w_1}{}^2 g_{n_2n_2}p_x\right)} \quad (S9)$$

$$\frac{\partial w_1}{\partial \alpha_1} = \frac{|H_{w_1}|}{|H|}$$

$$= \frac{-\lambda^2\alpha_1\alpha_2\left(f_{n_1w_1}f_{n_1} - f_{w_1}f_{n_1n_1}\right)\left(\alpha_2 p_{\mathrm{x}} g_{n_2}{}^2 + g_{n_2n_2}\left(\lambda + \alpha_1 p_{\mathrm{x}} f(n_1,w_1)\right)\right)}{\alpha_1{}^2\alpha_2\lambda^2\left[2\alpha_1 f_{n_1}f_{n_1w_1}f_{w_1}g_{n_2n_2}p_x - \alpha_1 f_{n_1}{}^2 f_{w_1w_1}g_{n_2n_2}p_x + f_{n_1w_1}{}^2\left(\lambda g_{n_2n_2} + \alpha_2 p_{\mathrm{x}} g_{n_2}{}^2\right) - f_{n_1n_1}\left(\lambda f_{w_1w_1}g_{n_2n_2} + \alpha_2 f_{w_1w_1}p_{\mathrm{x}}g_{n_2}{}^2 + \alpha_1 f_{w_1}{}^2 g_{n_2n_2}p_x\right)\right]}$$

$$= \frac{-\left(f_{n_1w_1}f_{n_1} - f_{w_1}f_{n_1n_1}\right)\left(\alpha_2 p_{\mathrm{x}} g_{n_2}{}^2 + g_{n_2n_2}\left(\lambda + \alpha_1 p_{\mathrm{x}} f(n_1,w_1)\right)\right)}{\alpha_1\left[2\alpha_1 f_{n_1}f_{n_1w_1}f_{w_1}g_{n_2n_2}p_x - \alpha_1 f_{n_1}{}^2 f_{w_1w_1}g_{n_2n_2}p_x + f_{n_1w_1}{}^2\left(\lambda g_{n_2n_2} + \alpha_2 p_{\mathrm{x}} g_{n_2}{}^2\right) - f_{n_1n_1}\left(\lambda f_{w_1w_1}g_{n_2n_2} + \alpha_2 f_{w_1w_1}p_{\mathrm{x}}g_{n_2}{}^2 + \alpha_1 f_{w_1}{}^2 g_{n_2n_2}p_x\right)\right]} \quad (S10)$$

Total differentiation of the first order conditions with respect to α_2 gives:

$[x]$ $\quad p_{\mathrm{x}}\frac{\partial \mathrm{x}}{\partial \alpha_2} - \frac{\partial \lambda}{\partial \alpha_2} = 0 \quad$ (S11)

$[n_1]$ $\quad \lambda\alpha_1 f_{n_1n_1}\frac{\partial n_1}{\partial \alpha_2} + \lambda\alpha_1 f_{n_1w_1}\frac{\partial w_1}{\partial \alpha_2} + \alpha_1 f_{n_1}\frac{\partial \lambda}{\partial \alpha_2} = 0$

$$[n_2] \quad \lambda \alpha_2 g_{n_2 n_2} \frac{\partial n_2}{\partial \alpha_2} + \alpha_2 g_{n_2} \frac{\partial \lambda}{\partial \alpha_2} = -\lambda g_{n_2}$$

$$[w_1] \quad \lambda \alpha_1 f_{w_1 n_1} \frac{\partial n_1}{\partial \alpha_2} + \lambda \alpha_1 f_{w_1 w_1} \frac{\partial w_1}{\partial \alpha_2} + \alpha_1 f_{w_1} \frac{\partial \lambda}{\partial \alpha_2} = 0$$

$$[\lambda] \quad \alpha_1 f_{n_1} \frac{\partial n_1}{\partial \alpha_2} + \alpha_1 f_{w_1} \frac{\partial w_1}{\partial \alpha_2} + \alpha_2 g_{n_2} \frac{\partial n_2}{\partial \alpha_2} - \frac{\partial x_1}{\partial \alpha_2} = -g(n_2)$$

The second order conditions can be expressed in terms of the Bordered Hessian representation as AH = B , where $A = \left[\frac{\partial x}{\partial \alpha_2}, \frac{\partial n_1}{\partial \alpha_2}, \frac{\partial n_2}{\partial \alpha_2}, \frac{\partial w_1}{\partial \alpha_2}, \frac{\partial \lambda}{\partial \alpha_2}\right]$ is the vector of derivatives of all endogenous variables w.r.t τ. H is the Hessian matrix shown below, and $B = \left[0,0,-\lambda g_{n_2}, 0, -g(n_2)\right]$.

$$H = \begin{bmatrix} p_{x_1} & 0 & 0 & 0 & -1 \\ 0 & \lambda \alpha_1 f_{n_1 n_1} & 0 & \lambda \alpha_1 f_{w_1 n_1} & \alpha_1 f_{n_1} \\ 0 & 0 & \lambda \alpha_2 g_{n_2 n_2} & 0 & \alpha_2 g_{n_2} \\ 0 & \lambda \alpha_1 f_{n_1 w_1} & 0 & \lambda \alpha_1 f_{w_1 w_1} & \alpha_1 f_{w_1} \\ -1 & \alpha_1 f_{n_1} & \alpha_2 g_{n_2} & \alpha_1 f_{w_1} & 0 \end{bmatrix} \quad (S12)$$

$$|H| = {\alpha_1}^2 \alpha_2 \lambda^2 \Big[2\alpha_1 f_{n_1} f_{n_1 w_1} f_{w_1} g_{n_2 n_2} p_x - \alpha_1 {f_{n_1}}^2 f_{w_1 w_1} g_{n_2 n_2} p_x + {f_{n_1 w_1}}^2 \left(\lambda g_{n_2 n_2} + \alpha_2 p_x {g_{n_2}}^2\right) - f_{n_1 n_1} \left(\lambda f_{w_1 w_1} g_{n_2 n_2} + \alpha_2 f_{w_1 w_1} p_x {g_{n_2}}^2 + \alpha_1 {f_{w_1}}^2 g_{n_2 n_2} p_x\right)\Big] \quad (S13)$$

$$\frac{\partial n_1}{\partial \alpha_2} = \frac{|H_{n_1}|}{|H|}$$

$$= \frac{{\alpha_1}^2 \alpha_2 \lambda^2 p_x \left(f_{n_1 w_1} f_{w_1} - f_{n_1} f_{w_1 w_1}\right)}{{\alpha_1}^2 \alpha_2 \lambda^2 \left[2\alpha_1 f_{n_1} f_{n_1 w_1} f_{w_1} g_{n_2 n_2} p_x - \alpha_1 {f_{n_1}}^2 f_{w_1 w_1} g_{n_2 n_2} p_x + {f_{n_1 w_1}}^2 \left(\lambda g_{n_2 n_2} + \alpha_2 p_x {g_{n_2}}^2\right) - f_{n_1 n_1} \left(\lambda f_{w_1 w_1} g_{n_2 n_2} + \alpha_2 f_{w_1 w_1} p_x {g_{n_2}}^2 + \alpha_1 {f_{w_1}}^2 g_{n_2 n_2} p_x\right)\right]}$$

$$= \frac{p_x\left(f_{n_1w_1}f_{w_1} - f_{n_1}f_{w_1w_1}\right)}{\left[2\alpha_1 f_{n_1}f_{n_1w_1}f_{w_1}g_{n_2n_2}p_x - \alpha_1 f_{n_1}{}^2 f_{w_1w_1}g_{n_2n_2}p_x + f_{n_1w_1}{}^2\left(\lambda g_{n_2n_2} + \alpha_2 p_x g_{n_2}{}^2\right) - f_{n_1n_1}\left(\lambda f_{w_1w_1}g_{n_2n_2} + \alpha_2 f_{w_1w_1}p_x g_{n_2}{}^2 + \alpha_1 f_{w_1}{}^2 g_{n_2n_2}p_x\right)\right]} \quad (S14)$$

$$\frac{\partial n_2}{\partial \alpha_2} = \frac{|H_{n_2}|}{|H|}$$

$$= \frac{\alpha_1{}^2 g_{n_2}\lambda^2\left[-2\alpha_1 f_{n_1}f_{n_1w_1}f_{w_1}p_x + \alpha_1 f_{n_1}{}^2 f_{w_1w_1}g_{n_2n_2}p_x - f_{n_1w_1}{}^2\left(\lambda + \alpha_2 p_x g(n_2)\right) + f_{n_1n_1}\left(\lambda f_{w_1w_1} + \alpha_1 f_{w_1}{}^2 p_x + \alpha_2 f_{w_1w_1}g_{n_2}p_x\right)\right]}{\alpha_1{}^2\alpha_2\lambda^2\left[2\alpha_1 f_{n_1}f_{n_1w_1}f_{w_1}g_{n_2n_2}p_x - \alpha_1 f_{n_1}{}^2 f_{w_1w_1}g_{n_2n_2}p_x + f_{n_1w_1}{}^2\left(\lambda g_{n_2n_2} + \alpha_2 p_x g_{n_2}{}^2\right) - f_{n_1n_1}\left(\lambda f_{w_1w_1}g_{n_2n_2} + \alpha_2 f_{w_1w_1}p_x g_{n_2}{}^2 + \alpha_1 f_{w_1}{}^2 g_{n_2n_2}p_x\right)\right]}$$

$$= \frac{g_{n_2}\left[-2\alpha_1 f_{n_1}f_{n_1w_1}f_{w_1}p_x + \alpha_1 f_{n_1}{}^2 f_{w_1w_1}g_{n_2n_2}p_x - f_{n_1w_1}{}^2\left(\lambda + \alpha_2 p_x g(n_2)\right) + f_{n_1n_1}\left(\lambda f_{w_1w_1} + \alpha_1 f_{w_1}{}^2 p_x + \alpha_2 f_{w_1w_1}g_{n_2}p_x\right)\right]}{\alpha_2\left[2\alpha_1 f_{n_1}f_{n_1w_1}f_{w_1}g_{n_2n_2}p_x - \alpha_1 f_{n_1}{}^2 f_{w_1w_1}g_{n_2n_2}p_x + f_{n_1w_1}{}^2\left(\lambda g_{n_2n_2} + \alpha_2 p_x g_{n_2}{}^2\right) - f_{n_1n_1}\left(\lambda f_{w_1w_1}g_{n_2n_2} + \alpha_2 f_{w_1w_1}p_x g_{n_2}{}^2 + \alpha_1 f_{w_1}{}^2 g_{n_2n_2}p_x\right)\right]} \quad (S15)$$

$$\frac{\partial w_1}{\partial \alpha_2} = \frac{|H_{w_1}|}{|H|}$$

$$= \frac{\alpha_1{}^2\alpha_2\lambda^2 p_x\left(f_{n_1w_1}f_{n_1} - f_{w_1}f_{n_1n_1}\right)\left(g_{n_2}{}^2 - g(n_2)g_{n_2n_2}\right)}{\alpha_1{}^2\alpha_2\lambda^2\left[2\alpha_1 f_{n_1}f_{n_1w_1}f_{w_1}g_{n_2n_2}p_x - \alpha_1 f_{n_1}{}^2 f_{w_1w_1}g_{n_2n_2}p_x + f_{n_1w_1}{}^2\left(\lambda g_{n_2n_2} + \alpha_2 p_x g_{n_2}{}^2\right) - f_{n_1n_1}\left(\lambda f_{w_1w_1}g_{n_2n_2} + \alpha_2 f_{w_1w_1}p_x g_{n_2}{}^2 + \alpha_1 f_{w_1}{}^2 g_{n_2n_2}p_x\right)\right]}$$

$$= \frac{p_x\left(f_{n_1w_1}f_{n_1} - f_{w_1}f_{n_1n_1}\right)\left(g_{n_2}{}^2 - g(n_2)g_{n_2n_2}\right)}{\left[2\alpha_1 f_{n_1}f_{n_1w_1}f_{w_1}g_{n_2n_2}p_x - \alpha_1 f_{n_1}{}^2 f_{w_1w_1}g_{n_2n_2}p_x + f_{n_1w_1}{}^2\left(\lambda g_{n_2n_2} + \alpha_2 p_x g_{n_2}{}^2\right) - f_{n_1n_1}\left(\lambda f_{w_1w_1}g_{n_2n_2} + \alpha_2 f_{w_1w_1}p_x g_{n_2}{}^2 + \alpha_1 f_{w_1}{}^2 g_{n_2n_2}p_x\right)\right]} \quad (S16)$$